Modifying the Fullerene Surface Using Endohedral Noble Gas Atoms: Density Functional Theory Based Molecular Dynamics Study of C70O3

Cite as:
Morrison, C., & Bil, A. (2012). Modifying the Fullerene Surface Using Endohedral Noble Gas Atoms: Density Functional Theory Based Molecular Dynamics Study of $C_{70}O_3$. *J. Phys. Chem A.*, 116(13), 3413-3419.

Manuscript received: 02/11/2011; Accepted: 12/03/2012; Article published: 26/03/2012

Modifying the Fullerene Surface Using Endohedral Noble Gas Atoms: Density Functional Theory Based Molecular Dynamics Study of $C_{70}O_3$**

Andrzej Bil[1,*] and Carole A. Morrison[2]

[1]Faculty of Chemistry, University of Wrocław, F. Joliot Curie 14, 50-383 Wrocław, Poland

[2]EaStCHEM, School of Chemistry, Joseph Black Building, University of Edinburgh, West Mains Road, Edinburgh, EH9 3JJ, UK.

[*]Corresponding author; e-mail: abil@elrond.chem.uni.wroc.pl

[**]This work has been performed under the HPC-EUROPA2 project (project number: 228398) with the support of the European Commission Capacities Area - Research Infrastructures Initiative. Work also made use of the EaSTCHEM Research Computing Facility (http://www.eastchem.ac.uk/rcf) and the Edinburgh Compute and Data Facility (ECDF) (http://www.ecdf.ed.ac.uk/). A.B. thanks the Ministry of Science and Higher Education, Republic of Poland, for supporting this work under the grant no. N N204 280738. Calculations with TURBOMOLE software were performed at Wroclaw Network and Supercomputing Center.

Supporting information:
Tables of numerical data plotted in Figures 4, 5, 7, and 8: interaction energies, volumes, bond lengths, energies, and enthalpies. This information is available free of charge via the Internet at http://pubs.acs.org

Graphical abstract:

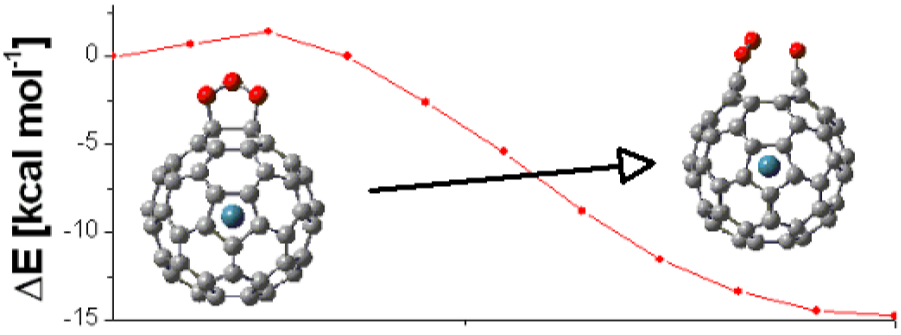

Keywords:
dispersion interactions, chemical reactivity, NEB, transition state

Abstract

We have performed a series of ab initio molecular orbital and molecular dynamics calculations to ascertain the influence of an endohedral noble gas atom on the reactivity of the surface of the model system $C_{70}O_3$. Our simulations show that the minimum energy pathways for the ozone ring-opening reaction are influenced by the presence of the endohedral atom. The effect is isomer dependent, with the enthalpy of the reaction increasing for *a*,*b*-$C_{70}O_3$ and decreasing for *e*,*e*-$C_{70}O_3$ when doped with the heavy noble gas atoms Xe and Rn.

I. Introduction

Groundbreaking work in the field of "chemical surgery" has opened up a new prospect for the chemistry of fullerenes that contain light molecules in their cages. Examples include reports on the insertion of an H_2 molecule into the C_{60} cage, and two H_2 molecules into C_{70},[1, 2]alongside other molecules such as CO, N_2, NH_3, and CH_4 (into open-cage fullerenes).[3-6] Single nitrogen atom and noble gas atoms have also been reported to penetrate and remain within $C_{60}$and C_{70} cages.[7-13] These achievements have triggered questions about the influence of the endohedral guest on the surface reactivity and properties of fullerene derivatives. Experimental data in this field are scarce. It has been observed, however, that in the range of 30–50 °C the equilibrium constant for the reaction of 9,10-dimethylanthracene (DMA) with C_{70}containing one or two H_2 molecules differed by as much as 15%,[2] and the analogous reaction with He@C_{60} returned an equilibrium constant that was noticeably larger than for Xe@C_{60}.[14]This latter result in particular seemed to be surprising: earlier theoretical work carried out on the large endohedral fullerene Y_3N@C_{78}[15] indicated that changes in the stress of the cage was a potential factor for altered surface properties, but in the case of the C_{60} encapsulation work the distances between pairs of C atoms (and therefore stress in the fullerene cage) do not change. This study therefore revealed that other factors must play a part, and suggested that the π-electrons from C_{60} could interact with the closed valence shells on Xe.

In this paper we undertook to determine the influence of the presence and identity of an endohedral noble gas guest (specifically, He, Ne, Ar, Kr, Xe, and Rn) on fullerene reactivity. We considered a range of properties that can be readily obtained in computational simulations and tried to find out which of them are influenced by the presence of the guest. The properties we considered included the relative stabilities of the isomers formed by a fullerene (due to the fact that not all C–C bonds are chemically equivalent), along with the enthalpy and energy barriers of a reaction where the fullerene or its endohedral derivative is involved. We have chosen $C_{70}O_3$ ozonide as a model system for our study, which is more challenging than a derivative of C_{60}.[16] C_{70} fullerene has five nonequivalent carbon atom types, which leads to eight nonequivalent types of bonds. Therefore, there are eight possible isomers of C_{70}fullerene monoozonides. The atoms are commonly labeled with letters from *a* to *e*, where *a*refers to apical carbon atoms and *e* labels carbon atoms in the equatorial belt (Figure 1). Two isomers, namely *a*,*b*-$C_{70}O_3$ and *c*,*c*-$C_{70}O_3$, are known experimentally[17] and are

the most stable ones computationally. The least stable isomer is *e*,*e*-$C_{70}O_3$, which has an energy ca. 31 kcal mol^{-1} higher than the *a*,*b*-ozonide.[16] The full set of possible C_{70} monoozonides therefore represents a good model to study how the presence of an endohedral guest influences the relative stability of the isomer series. Furthermore, it has been proven experimentally that C_{70}ozonides readily decompose, releasing molecules of O_2 to form the final stable oxide form.[17] We have studied this process previously, paying particular attention to the mechanism of ozone ring opening on the C_{70} surface.[16] The breaking of a C–C bond, which triggers the whole process, and the subsequent dissociation of an O–O bond is a simple model of a chemical reaction taking place on fullerene surface and is therefore ideally suited to our present investigation.

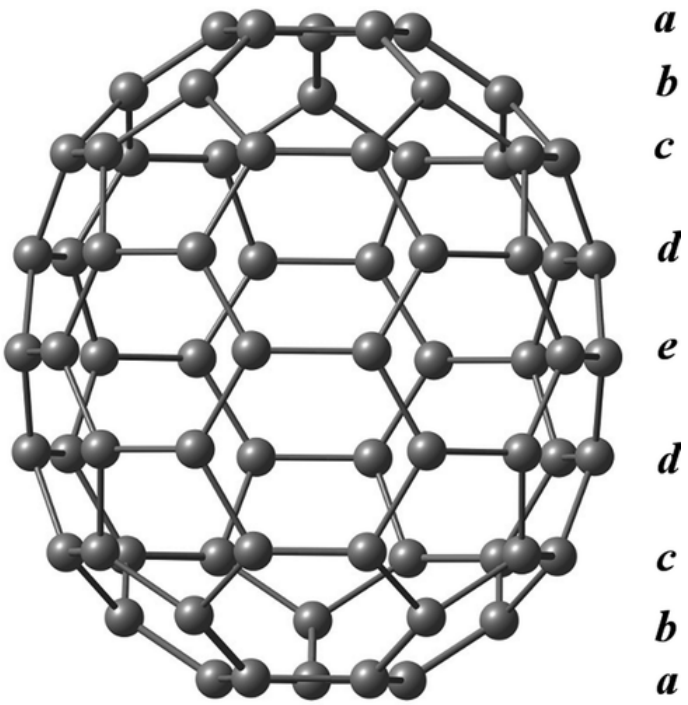

Figure 1. Eight nonequivalent carbon atoms in C_{70}.

In this study we shall perform a systematic theoretical study to determine what influence the identity of the endohedral atom has on the relative stabilities of the $C_{70}O_3$ isomer series and on the mechanism of the ozone ring opening on the fullerene surface. For this, two important factors have to be considered. First, noncovalent interactions between the noble gas atom and the carbon cage have to be described properly. Incorporation of van der Waals energy into density functional theory (DFT) is, however, not a trivial problem.[18, 19] For a long time the importance of van der Waals interactions in a proper description of a range of chemical and physical phenomena have been underestimated. For example, recent studies show that dispersion effects, which have been traditionally considered as a minor (or even negligible) contribution to the binding energy in ionic crystalline materials, are in fact critical to correctly account for the relative stabilities of the observed

phases.[20, 21] They are also needed to stabilize the tertiary structure of α-helices.[22] And of direct relevance to this work, dispersion corrections have been previously cited as important factors in studying the reactivity of fullerenes[23] and endohedrally doped fullerenes.[24]

The second factor we must consider is the fact that at nonzero temperatures atoms will explore the nonequilibrium parts of the potential energy surfaces. Thus, noble gas atoms can move inside a fullerene cage in different ways that are dependent on their masses and their interactions with carbon atoms, and in this way can modify the fullerene reactivity. The need to go beyond static calculations has been revealed in the diffusion Monte Carlo study of H_2 and $2H_2$ encapsulated in C_{60} and C_{70}.[25]

DFT-based molecular dynamics (MD) is a powerful first-principles computational method that allows the study of the behavior of a molecular system at a given temperature and allows us to investigate a chemical reaction as a process over a given time scale. In this study MD has allowed us to go beyond geometry-optimized static calculations, and to determine whether the endohedral guest influences the mechanism of ozone ring opening seen as a dynamical time dependent process. We also calculated relative stabilities of $C_{70}O_3$ isomers on the basis of time-averaged energies to supplement results obtained for equilibrium structures from static calculations.

II. Method

All calculations were performed using the Becke–Lee–Yang–Parr (BLYP) exchange–correlation DFT functional[26, 27] coupled to a dual localized (Gaussian) and plane-wave basis set description[28] as implemented in the QUICKSTEP program,[29] which is part of the CP2K suite of software.(30) Semiempirical dispersion corrections to BLYP energies and gradients have been calculated using the recently proposed DFT-D3 method.[31] For all elements we have used relativistic, norm-conservative Goedecker–Teter–Hutter pseudopotentials optimized for the BLYP functional.[32] Valence orbitals of the elements were expanded using double-ζ quality basis sets (specifically, DZVP-GTH-BLYP for C and Ne atoms, and MOLOPT for the rest of the noble gas atoms[33]). The auxiliary plane-wave basis set was defined by a cutoff energy of 300 Ry and applied to a cubic periodic boundary condition simulation cell of length 20 Å. The Born–Oppenheimer MD simulations were performed in the canonical ensemble (NVT), with a time-step of 0.7 fs and a chain of Nose–Hoover thermostats to regulate the mean temperature to 298 K. Transition states have been searched and minimum energy paths have been optimized using the improved tangent nudged elastic band (NEB) approach.[34] To further improve the values of the enthalpy and the energy barrier, we have performed single point energy calculations for the characteristic points on the minimum energy pathway at B3LYP-D3 level and def2-TZVPP[35] basis set, as implemented in TURBOMOLE.[36] For Xe and Rn atoms we used the recommended small-core relativistic pseudopotentials alongside a triple-ζ quality basis set.[37]

III. Results and Discussion

X@C_{70} Structure and Dynamics

Optimization of the C_{70} containing a heavy noble gas atom (>Ne) in its cage led to a structure where the endohedral atom tended to occupy a symmetric position at the center of mass of the carbon cage. For two light guests, He and Ne, the atom is essentially shifted toward one of the apex along the longer (polar) axis of the fullerene (Figure 2 upper panel, where t = 0 fs represents the geometry optimized structures). In Ar@C_{70} the noble atom is only slightly shifted from the mass center. As expected, introducing temperature into the simulation (298 K) led to small oscillations for the heavier atoms around the C_{70} mass center (Figure 2), and larger oscillations for the lighter He and Ne atoms—roughly between parallel planes defined by the d-type carbon atoms, as shown in Figure 3.

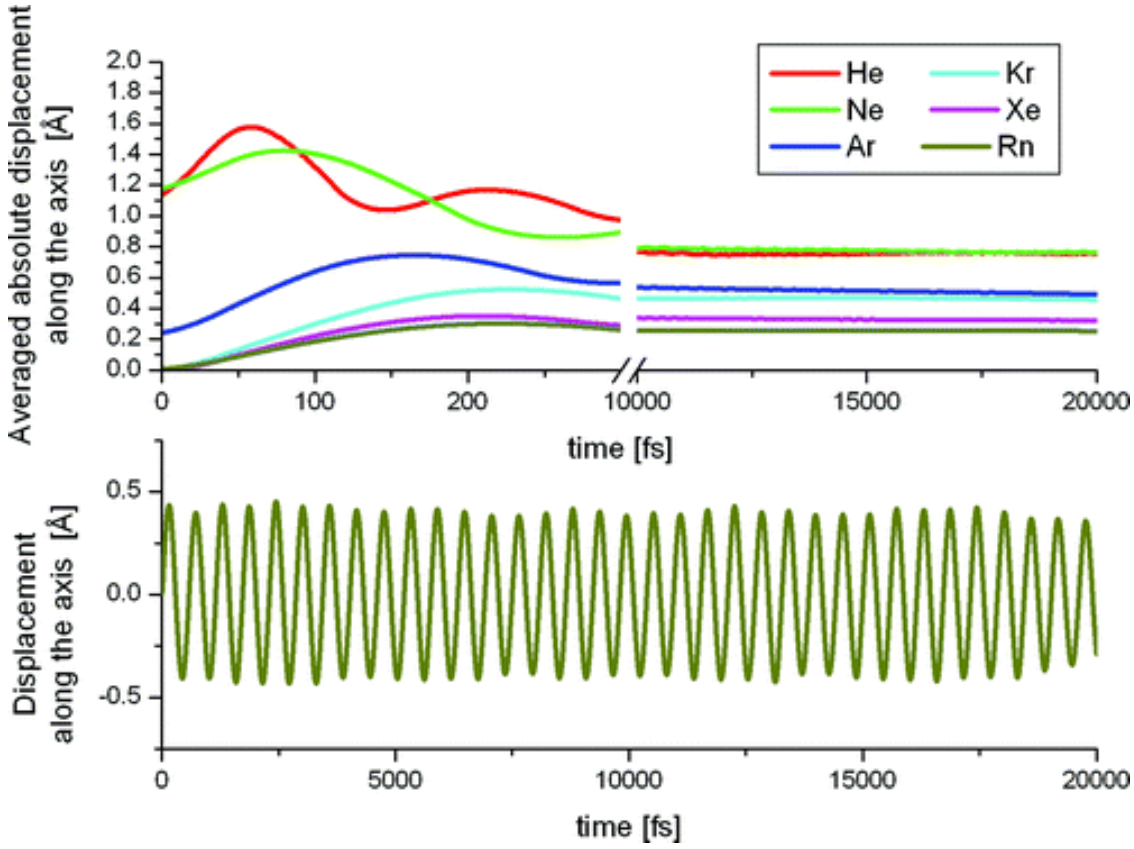

Figure 2. Time dependence of the displacement of the noble gas atom from the C_{70} mass center measured along the polar fullerene axis.

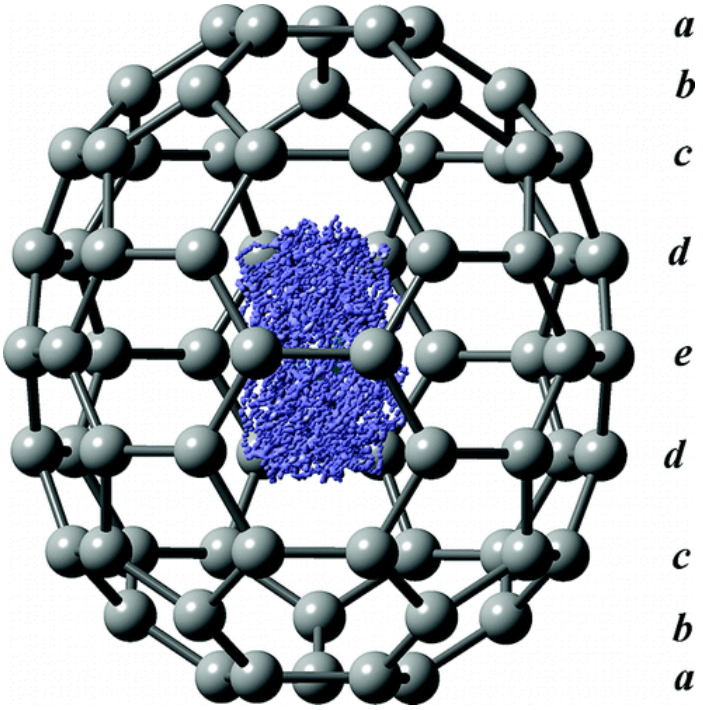

Figure 3. Trajectory (purple) arced by a He atom inside a C_{70} molecule during the course of a molecular dynamics simulation at 298 K.

The interaction energy (corrected for basis set superposition error[38, 39]) confirms that van der Waals interactions are critical for the proper description of X@C_{70} systems. The interaction energy between the noble gas atom and the carbon cage is always attractive and decreases monotonically from −1.5 kcal mol^{-1} for He@C_{70} to −21.7 kcal mol^{-1} for Rn@C_{70} (Figure 4 and Table S1 in the Supporting Information). When the calculations are carried out using the standard BLYP functional, which does not describe the dispersion interaction properly, the interaction energy is fully repulsive and increases up to 26.8 kcal mol^{-1}. The result is therefore unphysical, as it suggests that stable X@C_{70} molecules cannot be formed.

It is a matter of debate whether our reported numbers correctly reproduce the interaction energy between a noble gas atom and a C_{70} molecule, as there are no high-level reference data published so far, against which we could compare our results. Recently, reported DFT-SAPT data[40] suggest that the original DFT-D Grimme method[41] tends to overestimate the binding interaction energy between an encapsulated noble gas atom and a C_{60} cage, but the recent implementation of the semiempirical D3 dispersion correction, which is the one we have applied here, is expected to correct for this.[31]

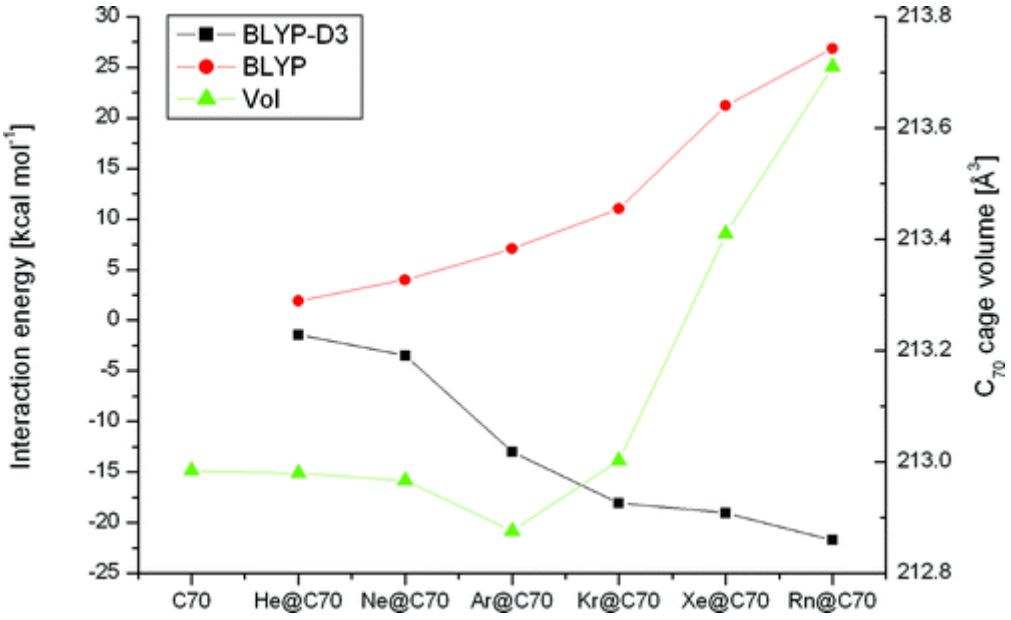

Figure 4. Left axis: calculated interaction energies between the C_{70} cage and the noble gas endohedral atom. Right axis: equilibrium volume of the carbon atom cage in C_{70} and X@C_{70}.

Our results also indicate that the presence of an endohedral guest has only a marginal influence on the equilibrium C–C bond lengths in the fullerene cage. A convenient parameter that allows us to analyze this effect is the volume enclosed by the cage (that is, the volume of the polyhedron established by the position of the carbon nuclei). Calculating the volume in this way returns a value of 213.0 $Å^3$ for the equilibrium structure of empty C_{70}, and this rises by only 0.7 $Å^3$ for Rn@C_{70} (Figure 4 and Table S2 in the Supporting Information). The changes in particular bonds lengths are listed in Table S2a, Supporting Information. As might be expected, the equatorial *e*,*e* bond is the most susceptible to change, and the largest changes are observed for the fullerenes doped with Xe and Rn. The elongation of this bond, however, does not exceed 0.006 Å. Ar@C_{70} is predicted to have a smaller internal volume than the empty cage, but again we stress that the numbers are small (ca. 0.1 $Å^3$). The situation does not change noticeably when we consider how the volume changes over the course of the ca. 20 ps MD trajectory, with the time-averaged volume of C_{70} and Rn@C_{70} predicted to be 213.6 ± 1.4 and 214.5 ± 0.9 $Å^3$, respectively.

The fact that the change in the average cage volume with respect to the noble gas identity is rather small can be misleading, as it may suggest that the interaction between the guest and the cage is negligibly small. The result is in fact the outcome of two opposing driving forces. Long range dispersion, which is always attractive and increases considerably with the noble atom size, leads to the volume shrinking. On the other hand, short-range Pauli repulsion between the noble gas atom and carbon atoms should lead to cage expansion. Thus the marginal increase in cage volume with Xe or Rn occupation suggests that electrons occupying the closed valence shells of the noble gas atom interact with the carbon atoms and slightly modify the electron structure

of C_{70}. These calculations therefore confirm the idea put forward by Frunzi, Cross, and Saunders that Pauli repulsion is a crucial element of interaction between an encapsulated noble gas atom and a fullerene.[14] They also reveal, however, that the dispersion interaction between the guest and the carbon cage is just as important. Both these factors may influence the properties and reactivities of endohedrally modified fullerenes, especially those doped with large polarizable atoms such as Xe and Rn.

Stability of the Ozonide Isomer Series

The relative stabilities of the equilibrium structures of the eight isomers of $C_{70}O_3$ are influenced only marginally by the presence of the endohedral noble gas guest (Figure 5 upper panel, Table S3 in Supporting Information). Data obtained for the $C_{70}O_3$ series of isomers (first column in Figure 5) are plotted versus the left vertical axis (ΔE). The change in relative energies as a function of the identity of the endohedral guest are so small that we present them as differences, expressed as $[E(X@i,j\text{-}C_{70}O_3) - E(X@(a,b\text{-}C_{70}O_3)] - [E(i,j\text{-}C_{70}O_3) - E((a,b\text{-}C_{70}O_3)]$, against the scale drawn on the right-hand axis ($\Delta\Delta E$). Typically, the changes in relative stability of the doped ozonide series are not larger than ±0.5 kcal mol^{-1} in comparison to the relative stabilities of isomers of empty $C_{70}O_3$, with the largest scattering of the values observed for Xe and Rn. Only for $e,e\text{-}C_{70}O_3$ are the changes more sensitive, increasing with the size of the noble gas atom until it reaches 2 kcal mol^{-1} for Rn.

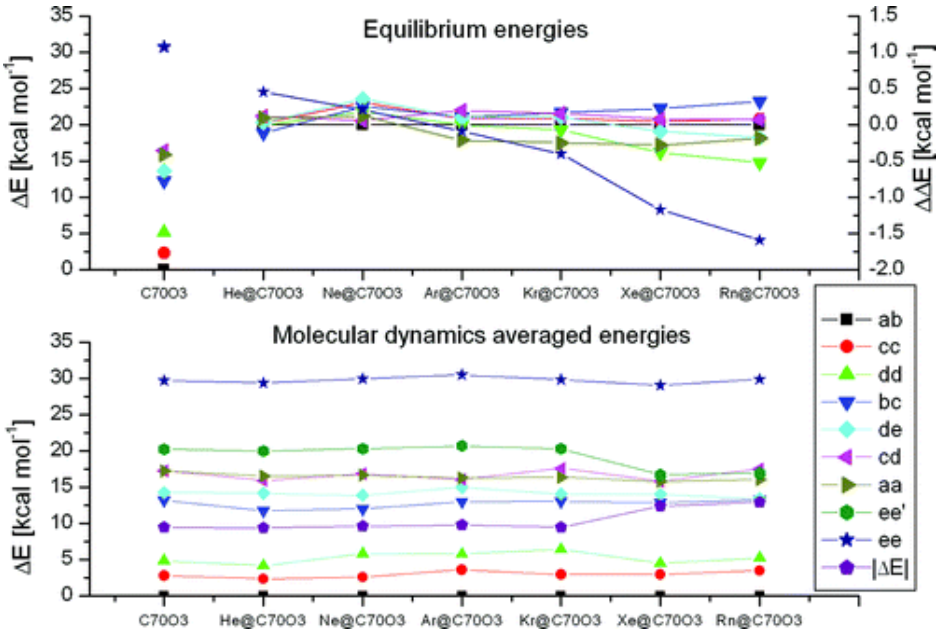

Figure 5. Total energies (upper panel) and average potential energies from MD trajectories (lower panel) of the $C_{70}O_3$ and $X@C_{70}O_3$ set of isomers, relative to the *a,b*- isomer. Due to small differences in relative energies for $X@C_{70}O_3$(upper panel), we mark the differences (right axis) between actual results for a given $X@C_{70}O_3$ and the relative stabilities of the isomers of $C_{70}O_3$ (left axis).

When the thermal factor is applied, and the atoms are able to explore the nonequilibrium parts of the potential energy surfaces, the influence of the identity of the guest on the relative stability of the isomers is much more pronounced, and it is no longer necessary to plot the results as relative differences (Figure 5 lower panel, Table S4 in Supporting Information). Average potential energies for the isomers can vary by up to 3 kcal mol^{-1} as the identity of X changes, but overall the stability order of the eight isomers is more or less maintained.

Mechanism of the Ozone Ring-Opening Reaction

The ozone ring-opening reaction for empty $C_{70}O_3$ is extensively discussed in ref 16. For all endohedrally doped *e*,*e*- isomers (that is, where the O_3 unit straddles two *e*,*e*-C atoms) we observed spontaneous ozone ring opening, which proceeds through a mechanism consistent with what we observed for the bare fullerene. This suggests that the chemical reaction is not influenced qualitatively by the presence of the guest. The first stage of the reaction involves breaking the C–C bond to which O_3 molecule is attached. This is then followed by a dissociation of the O–O bond, which leads the process to a new minimum. The whole process for He@*e*,*e*-$C_{70}O_3$ is summarized on a time line in Figure 6. Isomers other than X@*e*,*e*-$C_{70}O_3$ do not exhibit spontaneous ozone ring opening, in agreement with the set of empty ozonides. This result is important as it indicates that the noble gas guest does not substantially lower the potential energy surface barriers for the reaction scheme, a point we shall return to later in our discussion of our nudged elastic band (NEB) calculations.

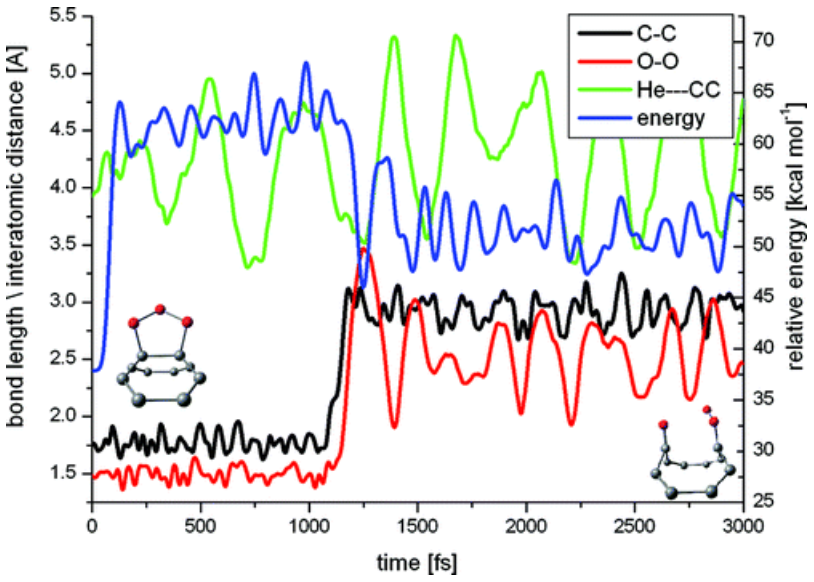

Figure 6. Selected parameters obtained from a section of the MD run performed for He@*e*,*e*-$C_{70}O_3$. The bond lengths C–C (black) and O–O (red), average distance between He atom and C atoms involved in the ozone ring (green), and the potential energy (blue) are depicted versus simulation time.

The green curve in Figure 6 represents an average distance between the He atom and the C atoms to which the O_3 unit is attached. The curve indicates that dissociation of the C–C bond takes place when the He atom approaches the C atoms, which may sugggest that the He atom does influence the process. Although the He atom may transfer some kinetic energy to the C atoms and in this way help to cross the energy barrier for C–C dissociation, the dynamic behavior of the guest atom is not a factor triggering the reaction (for instance, at t = 750 fs it also approaches the O_3 unit but this does not appear to result in any perturbation of the cage surface). The same mechanism is observed for all X@$C_{70}O_3$ species in the course of MD dynamics: movement of the noble gas atom does not correlate with the moment of C–C dissociation. Indeed, we observed some cases of C–C/O-O bonds dissociation where the X atom was departing from the C–C bond.

As discussed above, the ozone ring opening in the course of MD simulations for X@*e*,*e*-$C_{70}O_3$results in two different structures. The energy of the first structure, marked with a blue star (lower panel Figure 5), refers to the reactant where O_3 is attached to C_{70} at an *e*,*e*–C-C bond. The energy of the second structure (olive hexagon, marked *e*,*e*′) refers to the product of ozone ring opening. The difference between these values ($|\Delta E|$) is marked with a purple pentagon and represents the energy of the ozone ring-opening reaction (see also Table S4 in theSupporting Information). Interestingly, we observe that the process does show some sensitivity toward the noble gas atom identity, with $|\Delta E|$ for *e*,*e*-$C_{70}O_3$ doped with Xe and Rn around 3.0–3.5 kcal mol^{-1} larger than for the other considered structures.

As mentioned above, empty *a*,*b*-$C_{70}O_3$ and *c*,*c*-$C_{70}O_3$ do not undergo a spontaneous ring-opening process during the course of an MD simulation as the energy barriers are much higher that for *e*,*e*-$C_{70}O_3$.[16] In these cases improved tangent NEB calculations allowed us to find transition states for these reactions (Figure 7, Table S5 in Supporting Information). This technique allows us to drive the chemical reaction while optimizing the internal degrees of freedom of the system and therefore produce adiabatic potential energy surfaces. The calculations were performed with CP2K software with a density functional and basis set the same as for MD simulation, as described in the Method section. GGA-type functionals, such as BLYP, tends to underestimate reaction energy barriers. In our previous paper,[16] where we studied in detail the mechanism of ozone ring opening on the C_{70} surface, we improved the accuracy of calculated energy barriers by higher level method single point calculations for the transition state structures optimized with BLYP functional. The values calculated with hybrid B3LYP functional were in good agreement with experimental data. Here we employed a similar procedure. In the subsequent paragraphs (and in Table S5, Supporting Information), the energy values taken directly from NEB BLYP-D3 based calculations are followed by the number in parentheses representing B3LYP-D3 single-point result. As expected, the hybrid functional predicts higher energy barriers and higher reaction enthalpies.

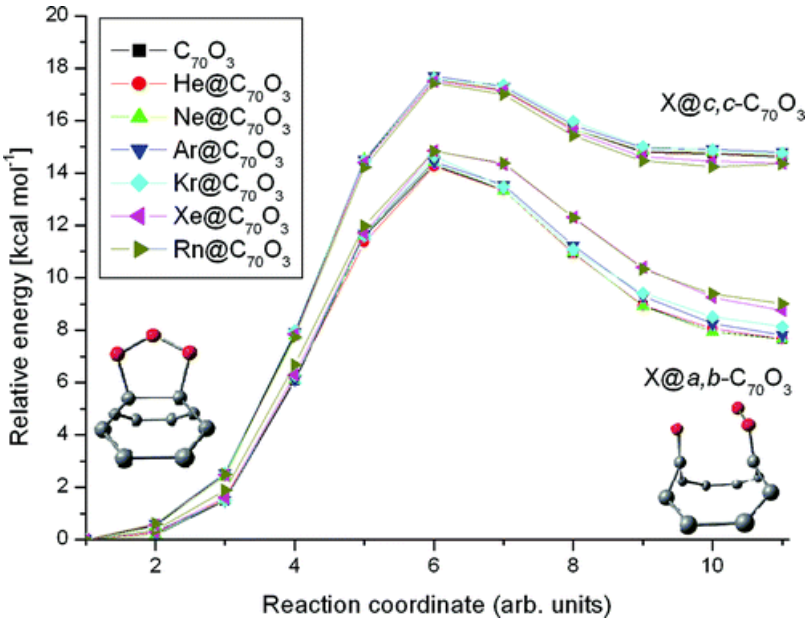

Figure 7. Minimum energy pathways calculated for X@*a*,*b*-$C_{70}O_3$ and X@*c*,*c*-$C_{70}O_3$. The path links minima on PESs related to closed and opened ozone rings on the fullerene surfaces.

The NEB results return energy barriers for the ring-opening reaction that are between 14.3 and 14.8 (21.6–22.3) kcal mol^{-1} for the X@*a*,*b*-$C_{70}O_3$ series and 17.4–17.7 (25.0–25.2) kcal mol^{-1} for the X@*c*,*c*-$C_{70}O_3$ series. For comparison we also performed similar calculations for the *e*,*e*-isomer series (Figure 8 and Table S5 in the Supporting Information) and obtained much lower barrier heights in the region of 1.4–1.8 (2.1–2.7) kcal mol^{-1}.

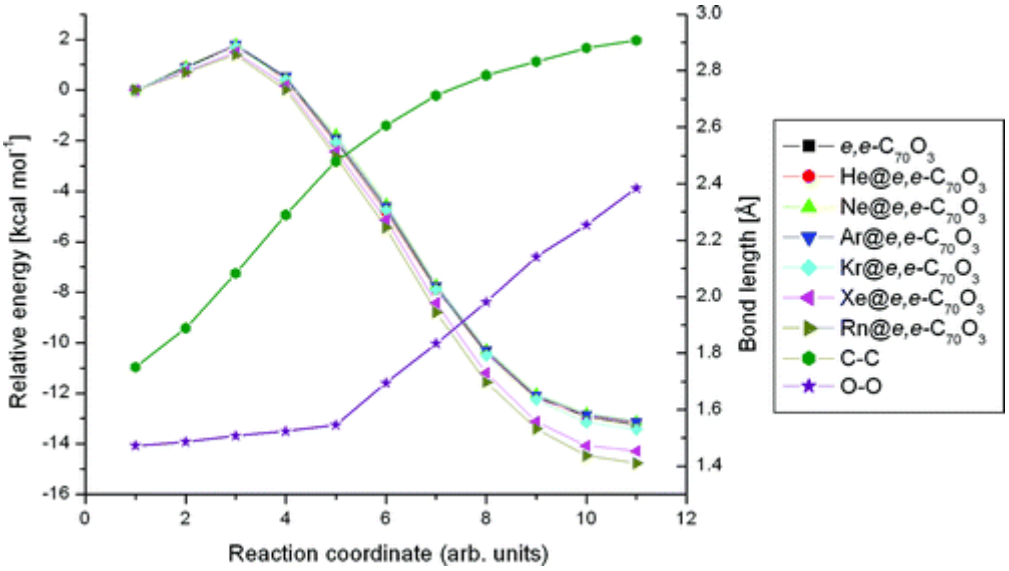

Figure 8. Minimum energy pathways as well as C–C and O–O bond distances calculated for X@*e*,*e*-$C_{70}O_3$.

In Figure 8 we also plot the C–C and O–O bond lengths for atoms involved in the ozone ring on the surface of Rn@*e*,*e*-$C_{70}O_3$ molecule. The evolution of the bonds length along the reaction path reveals a mechanism for the ozone ring opening that is consistent with the picture from the MD simulation. First, the energy of the system increases with the elongation of the C–C bond. At the transition state the C–C distance reaches 2.083 Å, which is considerably longer than for the initial equilibrium structure (1.750 Å). Contrary to that, the O–O distance is 1.507 Å, which is only slightly longer than equilibrium value (1.485 Å). Finally, dissociation of the O–O bond is accompanied by a decrease in the total energy of the system. The mechanism of the ozone ring opening observed in the NEB calculations is independent from the identity of an endohedral noble gas guest. The C–C and O–O bond lengths calculated for the transition state of the empty molecule (2.089 Å and 1.509 Å) are very close to the respective values reported above.

Values for ΔE for the ozone ring opening represents three different patterns depending on the isomers considered. For all members of the X@*c*,*c*-$C_{70}O_3$ series, the minimum energy path curves are almost independent of the identity of the X guest. In contrast, for X@*a*,*b*-$C_{70}O_3$ ΔEincreases with the size of the guest, from ca. 7.7 (ca. 10.2) kcal mol^{-1} (empty, He, Ne, Ar) to 8.8 (11.5) (Xe) and 9.0 (11.6) kcal mol^{-1} (Rn). For X@*e*,*e*-$C_{70}O_3$ we observe the opposite behavior: ΔEdecreases with the size of the guest from ca. −13.2 (ca. −10.5) kcal mol^{-1} (empty, He, Ne) to −14.3 (−11.3) kcal mol^{-1} (Xe) and −14.8 (−11.8) kcal mol^{-1} (Rn). (Note reported energies originate from minimum energy path optimizations and therefore do not contain zero point energy corrections.)

We have also made an attempt to determine whether the observed change in the enthalpy of the ring-opening reaction in X@*a*,*b*-$C_{70}O_3$ and X@*e*,*e*-$C_{70}O_3$ is simply a result of deformation of the fullerene skeleton due to the presence of a large endohedral guest. To this end, further calculations have been performed on the Rn@$C_{70}O_3$*a*,*b*- and *e*,*e*-isomer series, as we observed that the Rn atom has the biggest influence on the reaction pathway, and the most noticeable differences in the underlying PESs were observed for these isomer forms. In Figure 9 we compare the minimum energy pathways calculated for $C_{70}O_3$ and Rn@$C_{70}O_3$ with the plot marked as (Rn)@$C_{70}O_3$. Values for this plot have been calculated as a series of single-point energies for geometries taken from the Rn@$C_{70}O_3$ NEB calculations, but with the Rn atom removed. Or in other words, energies for each point were calculated for the $C_{70}O_3$ system deformed in such a way as to be able to accommodate a Rn atom inside the cage.

The results for the *a*,*b*-$C_{70}O_3$ isomer indicates that most points from the (Rn)@*a*,*b*-$C_{70}O_3$ curve coincide with the Rn@*a*,*b*-$C_{70}O_3$ minimum energy path. This proves that for this isomer the deformation of the fullerene due to the presence of noble gas guest is the leading factor that influences the ozone ring-opening reaction. However, the opposite conclusion can be drawn for the *e*,*e*-$C_{70}O_3$ isomer, where the curve (Rn)@*e*,*e*-$C_{70}O_3$ resembles the minimum energy path for empty *e*,*e*-$C_{70}O_3$ or even lies slightly above it. In this case it is not the pure cage deformation but the actual interaction between the Rn guest and carbon and oxygen atoms that

shifts the energy of the curve down and finally decrease the enthalpy of the ozone ring-opening process by around 1.5 kcal mol^{-1}.

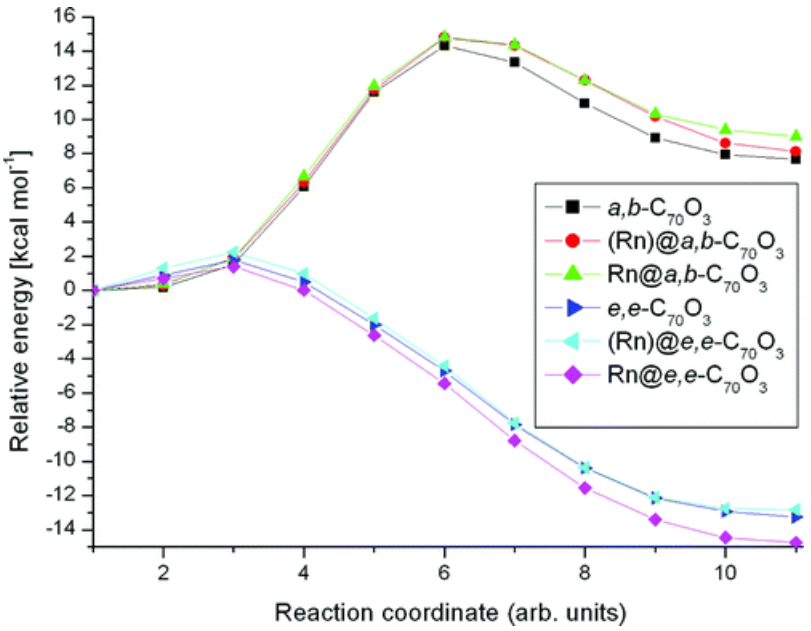

Figure 9. Minimum energy paths calculated for *a*,*b*- and *e*,*e*-isomers for empty $C_{70}O_3$ and Rn@$C_{70}O_3$, as well as $C_{70}O_3$ deformed as if the Rn atom were present inside the cage [(Rn)@$C_{70}O_3$].

IV. Conclusions

Thermally averaged positions of noble gas atoms inside the C_{70} cage coincide with the mass center of the molecule. At 0 K (equilibrium structure) the atom sits in the mass center only for heavier guests. The presence of the noble gas atom only slightly influences the volume of the carbon cage. In the case of Xe and Rn it does not imply, however, that the guest interacts negligibly with the fullerene. In fact, both dispersion (attraction) and Pauli (repulsion) forces can influence the fullerene properties and reactivity, but their near equal and opposite effects almost cancel each other out. Our results show that the relative stability of the $C_{70}O_3$ isomer series is influenced by the presence of the Xe or Rn guest. The most sensitive is the relative energy of the *e*,*e*-$C_{70}O_3$ isomer, which for the Rn doped molecule can be different from the empty one by up to 2 kcal mol^{-1} (0 K) or 3 kcal mol^{-1} (298 K).

The mechanism of the ozone ring opening on the surface of carbon cage, which can be observed spontaneously in a course of MD simulations for *e*,*e*-$C_{70}O_3$ only, is not influenced qualitatively by the presence of the guest. The minimum energy pathway of the process calculated for the endohedrally doped *a*,*b*-, *c*,*c*-, and *e*,*e*-isomers revealed, however, that the presence of Xe and Rn does influence the thermodynamics

of the reaction. The mechanism of that influence is not simple to explain by means of a single factor, such as a deformation of the fullerene cage, and the final result depends on the isomer considered. In the case of *c*,*c*-$C_{70}O_3$the enthalpy of ozone ring opening is insensitive on the noble gas guest. The enthalpy of the reaction increases when *a*,*b*-$C_{70}O_3$ is doped with Xe or Rn and decreases when the heaviest noble gas atoms are put into *e*,*e*-$C_{70}O_3$.

Results presented in this paper lead to the important conclusion that chemical processes taking place on the surface of fullerenes can be influenced by endohedral insertion of large guests such as a Xe or Rn atom, especially if the process involves C–C bond cleavage. Both the decrease and increase of the equilibrium constant can be expected depending on the type of C–C bond involved in the reaction.

References

[1] Komatsu, K.; Murata, M.; Murata, Y. *Science* **2005**, 307, 238-240.

[2] Murata, M.; Maeda, S.; Morinaka, Y.; Murata, Y.; Komatsu, K. *J. Am. Chem. Soc.* **2008**, 130, 15800-15801.

[3] Iwamatsu, Sho-ichi; Stanisky, C. M.; Cross, R. J.; Saunders, M.; Mizorogi, N.; Nagase S.; Murata, S. *Angew. Chem. Int. Ed*. **2006**, 45, 5337-5340.

[4] Whitener Jr., K. E.; Frunzi, M.; Iwamatsu, Sho-ichi; Murata, S.; Cross, R. J.; Saunders, M. *J. Am. Chem. Soc.* **2008**, 130, 13996-13999.

[5] Stanisky, C. M.; Cross, R. J.; Saunders, M. *J. Am. Chem. Soc.* **2009**, 131, 3392-3395.

[6] Whitener Jr., K. E.; Cross, R. J.; Saunders, M.; Iwamatsu, Sho-ichi; Murata, S.; Mizorogi, N.; Nagase, S. *J. Am. Chem. Soc.* **2009,** 131, 6338-6339.

[7] Almeida Murphy, T.; Pawlik, Th.; Weidinger, A.; Höhne, M.; Alcala, R.; Spaeth, J.-M. *Phys. Rev. Lett*. **1996**, 77, 1075-1078.

[8] Weiske, T.; Schwarz, H. *Angew. Chem., Int Ed.* **1992**, 31, 605-606.

[9] Saunders, M.; Jiménez-Vázquez, H. A.; Cross, R. J.; Poreda, R. J. *Science* **1993**, 259, 1428-1430.

[10] Saunders, M.; Jiménez-Vázquez, H. A.; Cross, R. J.; Mroczkowski, S.; Gross, M. L.; Giblin, D. E.; Poreda, R. J. *J. Am. Chem. Soc.* **1994**, 116, 2193-2194.

[11] Saunders, M.; Cross, R. J.; Jiménez-Vázquez, H. A.; Shimshi, R.; Khong, A. *Science* **1996**, 271, 1693-1697.

[12] DiCamillo, B. A.; Hettich, R. L.; Guiochon, G.; Compton, R. N.; Saunders, M.;. Jiménez-Vázquez, H. A; Khong, A.; Cross, R. J. *J. Phys. Chem* **1996**, 100, 9197-9201.

[13] Yamamoto, K.; Saunders, M.; Khong, A.; Cross Jr., R. J.; Grayson, M.; Gross, M. L.; Benedetto, A. F.; Weisman, R. B. *J. Am. Chem. Soc.* **1999**, 121, 1591-1596.

[14] Frunzi, M.; Cross, J.; Saunders, M. *J. Am. Chem. Soc.* **2007**, 129, 13343-13343.

[15] Osuna, S.; Swart, M.; Sola, M. *J. Am. Chem. Soc.* **2009**, 131, 129-139.

[16] Bil, A.; Latajka, Z.; Morrison, C. *J. Phys. Chem. A* **2009**, 113, 9891-9898.

[17] Heymann, D.; Bachilo, S.M.; Weisman, R.B. *J. Am. Chem. Soc.* **2002**, 124, 6317-6323.

[18] Grimme, S.; Anthony, J.; Schwabe, T.; Mück-Lichtenfeld, Ch. *Org. Biomol. Chem.* **2007**, 5, 741-758.

[19] Langreth D. C.; et al. *J. Phys.: Condens. Mattter* 21, **2009,** 084203.

[20] Bil, A.; Kolb, B.; Atkinson, R.; Pettifor, D. G.; Thonhauser, T.; Kolmogorov, A. N. *Phys. Rev. B* **2011**, 83, 224103.

[21] Wojtaś, M.; Bil, A.; Jakubas, R.; Gągor, A.; Pietraszko, A.; Czupiński, O.; Tylczyński, Z.; Isakov, D. *Phys. Rev. B* **2011**, 83, 144103.

[22] Shepherd, L. M. S.; Morrison, C. A. *J. Phys. Chem. B.* **2010**, 114, 7047-7055.

[23] Osuna, S.; Swart, M.; Sola, M. *J.Phys. Chem A* **2011**, 115, 3491-3496.

[24] Kruse, H.; Grimme, S. *J.Phys. Chem C* **2009**, 113, 17006-17010.

[25] Sebastianelli, F.; Xu, M.; Bačić, Z.; Lawler, R.; Turro, N. J. *J. Am. Chem. Soc.* **2010**, 132, 9826-9832.

[26] Becke, A. *Phys. Rev A* **1988**, 38 , 3098-3100.

[27] Lee, C.; Yang, W.; Parr, R. *Phys Rev B* 1988, 37, 785-789.

[28] Lippert, G; Hutter, J.; Parrinello, M. *Mol. Phys.* **1997**, 92, 477-488.

[29] Vande Vondele, J.; Krack, M; Mohamed, F; Parrinello, M; Chassaing, T; Hutter, J. *Comp. Phys. Commun.* **2005**, 167,103-128.

[30] The CP2K developers group, http://cp2k.berlios.de/

[31] Grimme, S.; Antony, J.; Ehrlich, S.; Krieg, H. *J. Chem. Phys.* **2010**, 132, 154104.

[32] Goedecker, S; Teter, M; Hutter J. *Phys. Rev. B* **1996**, 54, 1703-1710.

[33] Hartwigsen, C.; Goedecker,S.; Hutter, J. *Phys. Rev. B* **1998**, 58, 3641-3662.

[34] Krack, M. *Theor. Chem. Acc.* **2005**, 114, 145-152.

[35] VandeVondele, J.; Hutter J. *J. Chem. Phys.* **2007**, 127, 114105.

[36] Henkelman, G; Jonsson, H. *J. Chem. Phys*. **2000,** 113, 9978.

[37] Weigend, F.; Ahlrichs, R. *Phys. Chem. Chem. Phys.* **2005**, 7, 3297-3305.

[38] Ahlrichs, R.; Baer, M.; Haeser, M.; Horn, H.; Koelmel C. *Chem. Phys. Lett.* **1989**, 162, 165-169.

[39] Peterson, K. A.; Figgen, D.; Goll, E.; Stoll, H.; Dolg, M. *J. Chem. Phys.*, **2003**, 119, 11113.

[40] Boys S. F.; Bernardi F. *Mol. Phys.* **1970,** 19, 553-566.

[41] Mierzwicki K.; Latajka Z. *Chem. Phys. Lett.* **2003**, 380, 654-664.

[42] Hesselmann, A.; Korona, T. *Phys. Chem. Chem. Phys.* **2011**, 13, 732-743.

[43] Grimme, S. *J. Comput. Chem.* **2006**, 27, 1787-1799.